Journal of Optoelectronic and Biomedical Materials Vol. 16, No. 4, October-December 2024, p. 173-187

Synthesis, characterization and anticancer activity of zinc sulfide nanoparticle using heterocyclic Zn (II) thiosemicarbazone complex as a single source

R. Kothari*
Department of Chemistry, School of Sciences, ITM University, Gwalior (M.P.) India- 474005

The green synthesis of zinc sulphide nanoparticles (Zn S NPs) using Zn(II) complex as a single molecular precursor is gaining importance due to its simplicity, cost – effectiveness and pharmacologically active nature. Now – a- day's nanobiotechnolgy is increasing at a fast rate due to its many possible applications in the biomedical and, pharmaceuticals fields. In this paper, we have reported the synthesis of Chalcogenide nanostructured pharmacologically active Zn S nanoparticles using Zn (II) Heterocyclic thiosemicarbazone Complex as a Single Source. Zn (II) complex was synthesized by the reaction between Schiff base ligand and Zinc acetate salt in 2:1 molar ratio. Thiosemicarbazone have a wide clinical antitumor spectrum with efficacy in various tumor types such as leukemia, pancreatic cancer, breast cancer, non- small cell lung cancer, cervical cancer, prostate cancer and bladder cancer. These compounds possessed significant antineoplastic activity when the carbonyl group attachment of the side chain was located at a position alpha to the heterocyclic nitrogen atom, whereas attachment of the side chain β or gamma to the heterocyclic nitrogen atom, resulted in inactive antitumor agents. In addition, replacement of the heterocyclic ring N with carbon also resulted in a biologically inactive compound suggesting that a conjugated N, N, S -tridentate donor set is essential for the biological activities of thiosemicarbazone ligands. In our study, for synthesis of Zn S nanoparticles, the synthesized Zn(II) complex of thiosemicarbazone ligand was treated with aqueous extract of Parmotrema perlatum flowers. The use of aqueous extract of Parmotrema perlatum flowers in the synthesis of ZnS particles plays a very important role in reducing reaction time, reducing minimum possibility of side reactions and conversion of metal complexes into its nanoparticles in a very less time. All synthesized compounds were characterized by various structural, morphological, electronic and vibrational spectroscopic techniques and also evaluate the pharmacological activities of compounds like antioxidant, anti-inflammatory and anticancer activities. The peaks at 3414.82 cm^{-1} in FT-IR spectra confirms the presence of –OH groups and other bioactive agents in the aqueous extract of Parmotrema perlatum flowers, which acts as a capping and stabilizing agents in the synthesis of Zn S nano particles. The effective results of anti-cancer activity of compounds showed that the ZnS nanoparticles shows good cytotoxic activity against human breast cancer cell lines (MCF-7) using MTT assay. In this study, normal human cell lines used as standard for comparison purpose. The CTC_{50} values of ZnS nanoparticles was found to be 49.375µg/ml respectively. Therefore, it could be concluded that this biogenic method is effective for synthesis of Zn S nanoparticles from Zn(II) complex with desirable properties for potential biomedical applications which can be consider as a good drug candidate for anti-cancer therapy.

(Received June 7, 2024; Accepted October 8, 2024)

Keywords: Zinc complex, Zn S nanoparticle, Structural and morphological characterization, Anticancer activity, Antioxidant activity

1. Introduction

Green chemistry for the sustainable development of nanomaterials has gained greater interest in the last few decades with researcher's aim to reduce hazards through development of

* Corresponding author: richakothari@itmuniversity.ac.in
https://doi.org/10.15251/JOBM.2024.164.173

greener methods for biosynthesis of nanomaterials using plants as one simple and ecofriendly approach. It is one of the simple and ecofriendly approach for synthesis of nanomaterials. [1].

In principle, the synthesis of nanostructures demands a selection of

a) Suitable solvent

b) a good reducing agent

c) a good stabilizing agent.

Previously various chemical methods can be applied for the synthesis of nanoparticles, out of them plant medicated green approach is considered as safe, ecofriendly, and lowcost method. Therefore, plant mediated synthesis of nanomaterials has become an innovative industrial technique with lots of benefits due to plant obtainability and less expensive, use of ess hazardous and less expressive chemicals,and scalding up possibility, and the nanomaterials obtained with desirable size and shape tailorability [2,3].

Green synthesis of nanoparticles basically involves the use of plant extracts to reduce and stabilizing metal ions through some implicated plant phytochemicals like alkaloids, amino acids, enzymes, saponins, terpenoids, phenolic [4,5].

Transition metal chalcogenides are important semiconductor materials that have continued to draw attention due to their outstanding properties and wide range of [6,7] industrial applications in diverse fields. Specially, ZnS is a II-IV semiconductor that has continued to gain more attention owing to industrial, biological and agricultural applications [8]. The nanoparticles show significant quantum confinement effects that influence their optical and electrical properties [9]. Hence, its application in photo voltaics, photonic/ optoelectronic devices, sensors and catalysis [10,11]. ZnS is a promising semiconductor with a wide band gap, which benefiting electronic, optoelectronic, and electro chemical devices [6]. ZnS nanoparticles commonly show distinct features different from its bulk counterpart as a result of high surface- to- volume ratio [7]. It can be synthesized by various methods such as physical, chemical, and biological approaches [8-10]. While physical pathways such as thermal evaporation [11], pulsed laser vaporization [12] and molecular beam epitoxy [13] and chemical methods like coprecipation [14], sol gel [9], sonochemical [15] and hydrothermal [10] are widely employed, biosynthesis is still in its advent. In addition to this, the conventional physical and chemical methods are expensive and release hazardous materials into the environment [16]; hence, to reduce such risk, green synthesis has been considered the most reliable and safe method. Furthermore, green synthesis has become preferred as it is quick and suitable for large scale production, with plant-based extract being most applicable for NPs size and shape control as driven by their phytochemical compounds [17,18,19]. Biological activity studies on ZnS nanoparticles have reported significant action against large no of test bacteria, being more effective on gram- positive bacteria, and nontoxic against human erythrocytes [20].

A large number of studies have illustrated the feasibility of using plant materials like seed, leaves, and roots as a capping, reducing and stabilizing agent in the green synthesis of nanomaterials with certain properties and applications [21,22, 23]. In this regards, ZnS nanoparticles have been the subject of many plant-based biosynthesis studies, of which Parmotrema perlatum extract based green synthesis was a promising route. Parmotrema perlatum commonly known as black stone flower, is a spices of lichen used as a spice in India. In Ayurvedic stone flower is renowned for its potent ability to eliminate kidney stones from the renal system and uplift renal functions. Moreover, it supplies tremendous merits for wound –healing when applied as a topical herbal formulation, thanks to its strong antimicrobial and anti -inflammatory traits. Displaying superb capabilities in balancing the exacerbated Kapha and Pitta dosh,besides relieving asthma symptoms and curing respiratory illness owing to its decongestant qualities. Stone flowers is undoubtedly a panacea from mother nature for alleviating myriad health woes. To the best of our knowledge, green synthesis of Zn S nanoparticles using aqueous extract of Parmotrema perlatum flowers and pharmacological evaluation of their cytotoxic studies, are not well documented. Therefore, the main objective of this work is to utilize aqueous extract of parmotrema perlatum flowers for the synthesis of ZnS NPs and to investigate their physicochemical and biological properties. The biogenic ZnS NPs were characterized for their structural properties using FT-IR, XRD, SEM and UV-visible and for their bioactivity using anti-oxidant and anticancer activity.

2. Experimental

2.1. Materials and physical measurements

All the reagents used in this study were of analytical grade, were purchased from sigma-Aldrich chemicals compound company and were used without any further purification. These include 4- nitroacetophenone thiosemicarbazide, hydrochloride, Dimethylsulphoxide, Zinc acetate dehydrate, methanol, cyclohexane diethyl ether, DPPH. The percentage elemental composition (C, H, N and S) of the complex was estimated using an Elemental analyzer various EL cube, Infra-red spectra obtained at room temperature, were carried out a Perkin Elmer, FTIR spectra photometer SAIF, ITM University Gwalior, in the wavelength range of 4000 – 400 cm^{-1}. The Nuclear magnetic resonance (NMR)spectra were recorded on a 600 MH_Z Bruker Avance III NMR Spectrometer: for H^1 NMR analysis in deprotonated chloroform solution ($CDCl_3$). Powder X-ray diffract gram (XRD) of the nanoparticles was recorded on a Bruker D8 Advanced XRD machine equipped with a proportional counter using CuK∝ radiation (ʎ=1.5405A°nickle filter), samples were added on a feat steel sample holder and scanned from 10 to 80ºc. The diffraction peak at several values were matched with other recorded standard in JCPDS card Ultraviolet visible(UV-Vis) spectra of the nanopartiicles were recorded using a Perkin Elmer, Lambda 25 spectrophotometer in SAIF, PC ray research Centre, ITM University Gwalior, in the range of 200-900 nm, using a 1cm path length cell with dichromethane solvent. Melting point of ligand and its Zn complex were obtained by an electro thermal melting point apparatus using open capillary method and were not corrected due to atmospheric condition of laboratory. Thermo Flash EA - 1112 series at the temperature up to 900ºc and vanadium pentaoxide (V_2 O_5) was used as an oxidizer to prevent inhibition caused by sulfur present in the compound. Thin layer chromatography (TLC) was performed using n-hexane/ EtoAc (1:3) ratio as an elutant. Distilled water was used in all experimental procedures.

2.2. Synthesis of substituted N^4 thiosemicarbazone ligand (L)

Substituted N^4 thiosemicarbazone ligand (L) has been synthesized as described by Zeglis B.M. et al [24] by reaction between 4-nitroacetophenone and thiosemicarbazide hydrochloride in a 1:1 molar ratio (scheme 1). The solution of thiosemicarbazide (0.911g,10mmol) was prepared upon stirring and heating it in 30 ml ethyl alcohol (96%V/V). 4 nitroacetophenol (1.65g,10mmol) was then added to the obtained colorless solution. As a result, a light-yellow solution was obtained. It was heated (80°c) with constant stirring for 1 hour. A pale-yellow precipitate has been formed upon cooling of the reaction mixture. It was separated by filtration, washed with cold ethanol and dried in vacuo.

Pale yellow solid, yield: 87%, pt. 160-161°c: FW: 238g/mol; Anal.calc. for C_9 $H_{10}O_2N_4S$; C,54.50; H;5.46; N,24.93; S,14.52%, Found; C, 54.39; H,5.30; N, 25.60; S, 14.30%. Main IR peaks (cm^{-1}); ν(NH) 3366;3142; ν (C=C) 1642, ν (C=N) 1602, and ν (C=S) 1314.

H^1 NMR (acetone-d6; δppm): 10.76 (broad, ^{1}H, NH); 8.62 (s, ^{1}H, CH, aromatic); 8.59 (broad, ^{1}H, NH); 8.24 (S, H, CH=N); *.11 (d, CH aromatic); 7.80 (t, ^{1}H, CH aromatic); and 4.36 (m, 2H, C-N).

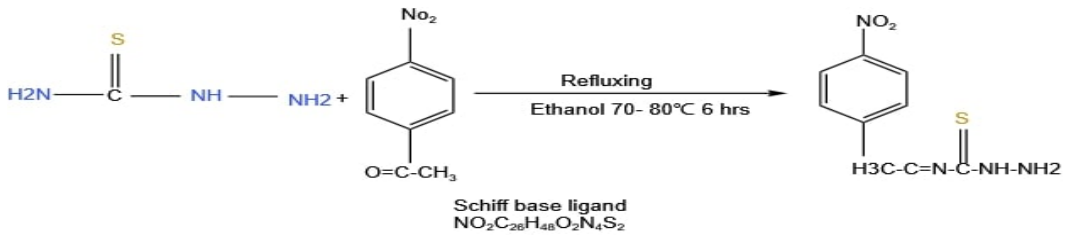

Scheme 1. Synthesis of Substituted N^4 thiosemicarbazone ligand (L).

Fig.1 Image of synthesis of substituted N^4 thiosemicarbazone ligand (L).

2.3. Synthesis of Zn(II) Complex: [Zn $(L)_2$ Cl_2]

Substituted N^4 –Thiosemicarbazone ligand (L) 1.03g, 5mmol) was dissolved in 25 ml of ethanol upon heating (160 ºc). After that, a sample of solid zinc chloride ($ZnCl_2$) (0.274g,5mmol) was added to the hot solution. The resultant reaction mixture was stirred for 60 minutes at 60-70ºc. The yellow precipitate of Zinc (II) Complex was obtained upon cooling to room temperature. It was filtered out, washed with cold ethanol, and dried in vacuo.

Yellow solid yield 72%; FW =581.38g/mol; Anal.calc. for [Zn (C_{18} H_{21} N_8 O_4 S_2)$_2$ Cl $_2$]; C=35.50; H,3.86; Cl,10.49; N, 16.58; s,9.49; Zn,19.36

Found, 35.37; H,3. 92; cl, 10.56, N,16.68; s, 9.75; Zn ,19.48.

Main IR peaks (cm^{-1}). ν (NH- 3183), ν (C=C)1642, ν (C=N) 1597, ν (C-S) 756. µeff. (293±1k) 0µB; Molar conductance (CH_3OH); –(55 Ω^{-1} cm^{-1} $mol^{-1.}$

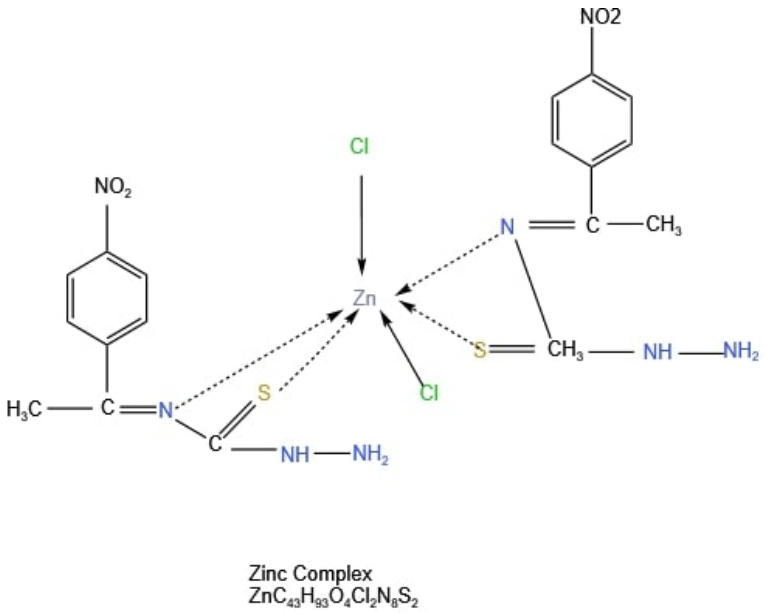

Scheme 2. Synthesis of Zn(II) Complex: [Zn $(L)_2$ Cl_2].

Fig.2 Image of synthesis of Zn (II) Complex: [Zn (L)$_2$ Cl$_2$].

2.4. Green synthesis of ZnS nanoparticles

Using synthesized for Zn(II) complex as a single source precursor. The ZnS nanoparticles were synthesized with slight modifications of an established green procedure, using a synthesized single source precursor of Zn (II) complex [25, 26]. About 0.3g of the complex was dispersed in 5 ml of dimethyl sulphoxide solvent (DMSO) and injected into an aqueous extract of Parmotrema perlatum flowers (25ml) at room temperature with vigorous stirring. The reaction temperature was maintained at room temperature while aliquots were taken at 15, 30 and 45minutes, to monitor the growth of formation of ZnS nanoparticles. After 60 minutes, the stirring was stopped and the solution was allowed to cool to room temperature, then excess of methanol was added to precipitate the nanoparticles. The solid was separated by centrifugation technique and re-dispersed in methanol. The centrifugation and isolation procedure were repeated three times for the purification of nanoparticles. The synthesized nanoparticles were represented as Zn S NPs.

Table 1. Physiochemical properties of ligand and its Zn (II) complex

S. N.	Compound	Colour	Melting point	Molecular weight	Molar Conductance	Analysis(%) Found				ʎ Max
						C%	H%	N%	Cal. Cu%	
1.	Schiff base ligand [$C_9H_{10}O_2N_4S$]	Pale Yellow	160-161°c	238	-	54.50 (54.93)	5.46 (5.30)	24.93 (25.60)	-	320nm
2	[Zn(C_{18} H_{21} N_8 O_4 S_2 Cl0 $_2$] Complex	Dark Yellow	200±2º c	581.38	55	(35.50),	5.0 (4.84)	9.12 (9.05)	7.46 %	215nm

2.5. Biological/ pharmacology

2.5.1. Evaluation of anticancer activity via MTT assay

MTT assay is a colorimetric assay for determination the cellular growth which reduced the tetrazolium yellow dye (MTT) to an insoluble formazan of purple colour, by the process of mitochondrial dehydrogenases of living cells. Generally, MTT assay is used for determination of cytotoxicity of drug and newly prepared other compound (39.40). Breast cancer human cell lines (MCF-7) along with normal cells (PBMCS) were maintained at RPMI-1640 culture media that was supplemented with 10% inactivated fettle serum (FCS) and antibiotic solution. These cells were plated with density of 5×10^3 cells per well in a 96 well plate and cultured for 24 hours at 37° c stock solution of test compounds were prepared in an equimolar mixture of DMSO and tetrahydrofuran (THF). All the cells were successively exposed to ligand, Zn (II) complex and ZnS

nanoparticles. The cell proliferation was measured by addition of 20µl of MTT dye (5mg/L in phosphate buffer saline) per cell after 48hrs incubation of the plates. These plates were further incubated for additional 4 hours, at 37°c in a humidified chamber with 5% CO_2. On the reduction of dye by effect of viable cell in each well that was dissolved in 150µl DMSO, the purple formazan crystals were produced and the absorption was noted at 570nm.The value of absorption were calculated in the form of % cell viability with accordance to the control group taken as 100%. The concentration of test compound required for 50% inhibition of cell viability is commonly termed as IC_{50} calculated by graph pad "Prism3.0" software [27].

2.5.2 Evaluation of antioxidant activity of compounds

Free radical scavenging ability was performed according to modified Brand-Williams protocols as described previously[28]. Freshly prepared stock solution (1mg/ml) of ligand Zn(II) complex and Zn S nanoparticles were diluted to a final concentration of 5, 10,15 and 20 µg/ml in DMSO. The methenolic solution of DPPH (2,2- diphenyl-1-picrylhydrazyl) (1ml. 0.3 mol m) was mixed in a beaker with 3.0 ml of ligand , Zn(II) complex and Zn S nanoparticles of above mentioned concentration. Meanwhile methanol (1ml) was added with test sample (3.0ml) for the preparation of blank solution. Negative control was made up of DPPH solution (1ml) and 3ml DMSO solvent. The solution was kept at a room temperature for at least 30 minutes, and then absorption was recorded at 517nm. Percentage scavenging ability of test compounds were calculated with the help of following equation.

$$\% \text{ RSA} = Ac - As/Ac \times 100$$

2.5.3. Evaluation of anti-inflammatory activity of compounds

The reaction mixture (0.5 mL) consisted of 0.45 ml Bovine serum albumin (3% aqueous solution) and varying concentration of compounds (25, 50, 75, 100 µg/mL of final volume). pH were adjusted to 6.3 using small amount of 1 N hydrochloric acid. The samples were incubated at 37° C for 20 min and then heated at 80° C for 2 min. After cooling the samples, 2.5 mL phosphate buffer saline (pH 6.3) was added to each tube. The absorbance was measured using UV-Visible spectrophotometer at 416 nm. Diclofenac sodium, an anti-inflammatory drug is used as a standard drug. The experiment was performed in triplicate. Percentage inhibition of protein denaturation was calculated as follows:

Percentage inhibition % = [(Abs(control) - Abs sample)/Abs(control)] X100

Abscontrol = Absorbance of blank sample

Abs(sample) =Absorbance of synthesised compounds

3. Result and discussion

The thiosemicarbazide ligand (L) has been previously described by Zeglis B.M. et al. [29] and has been obtained using the described method. Its yield is 87%, It was characterized by FT-IR, UV-Visible, H ^{1} NMR spectroscopy. Also, its particle size has been determined using X-ray diffraction analysis. The Zn(II) complex synthesized by ligand and Zinc chloride salt in a 2:1 molar ratio. The composition of the ligand and its Zn (II) complex has been confirmed using elemental analysis.

3.1. Study of substances in a solid state

3.1.1. Structural characterization of ligand, its Zn (II) and Zn S nanoparticles

The X-ray structures of Zn S nanoparticles are presented in fig.1.

The conformation of ligand, which differ only by position of nitrogen atom N (4) in benzene ring, are nearly the same as previously synthesized ligand. In complex the ligand (L) acts as neutral tridentate around the zinc (II) ions, respectively through an SNN set of donor atoms. Deprotonation of N- atom in ligand has led to the decrease of N-C bond distance. The longer Zn- S bond interactions and the acute chelate angles seemed to be the major contributors to the distortion

of the 4+1 coordination geometry. Therefore, the geometry around the Zn atoms was distorted trigonal bipiramidal with about 35% along the Berry pseudo rotation. In a complex, the Zn atom was bonded to the thiosemicarbazone ligand through the two S atoms and to the zinc ions through two nitrogen atoms of the Lewis base, to form Zn S_4N_2 group in a complex. To inspect the purity and crystal nature of the biogenic ZnS nanoparticles XRD analysis was performed and the data obtained were depicted in figure 1- compared with the standard spectral [JCPDS card no: 05-0566]. The results indicate cubic crystalline structure and, according to Scherrer's formula [30]. The average particle size of Zn S nanoparticle was 2.36. The resulted of XRD analysis are comparable to some other synthesized ZnS NPs [31] for example, the D value calculated by XRD method for ZnS NPs obtained by, e.g. sol gel (29.0nm) [9], prepare HY/ (an alkyl ammonium salt: 4.8 nm) [32], solid state (4.6), glucose mediated (5.3) [33], starch – capped (3.3) [34], polyvinyl alcohol (2.9) [35], and uncapped (3.7nm) [36] were close to obtained one of 2.4nm.

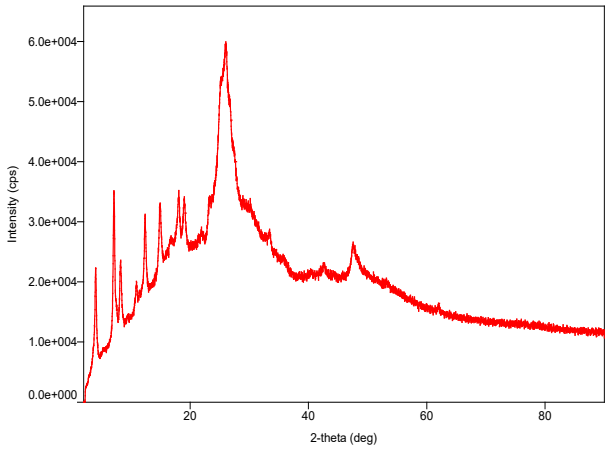

Fig.3. Powdered XRD spectra of Zn S nanoparticles.

3.1.2. Infrared spectra

FT-IR analysis is a very significant and reliable technique for the identification of synthesis of nanomaterials. The process of formation of complex leads to the appearance of a number of changes in the IR spectrum in comparison with the IR spectrum of the free ligand.A change in the position of the ν (C=N) band in the IR spectrum of complex due to the presence of functional groups. The absorption bands of Zn(II) appeared at 3446,1624,962 & 662 cm^{-1} .Similarly, the absorption bands of Zn S nanoparticles appeared at 2985,2414,1570,664 and 402 cm^{-1} .In a complex the ν (C=N) band is shifted by 18-46 cm^{-1} towards lower wave number comparing with the free ligand L (1642cm^{-1}). All the above changes indicate [37] that the azomethine nitrogen atoms as well as the sulfur atoms of the thiosemicarbazone ligand are involved in the coordination process. The major changes appeared in the FT-IR spectra of Zn S nanoparticles due to the bio reduction of Zn (II) complex into Zn S nanoparticles because phytochemicals act as both stabilizing agent as well as capping agent.

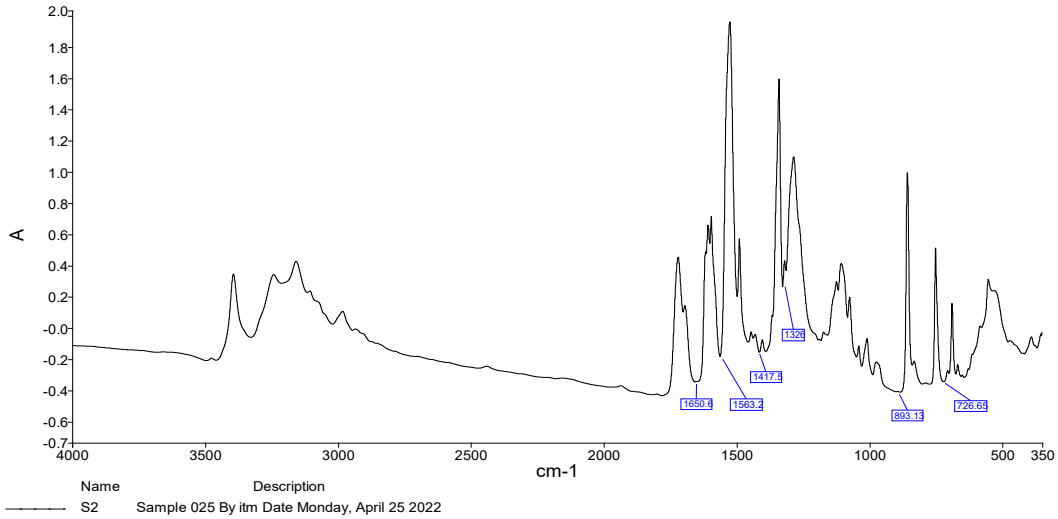

Fig. 4. FT-IR Spectra of Zn(II) complex of thiosemicarbazone ligand.

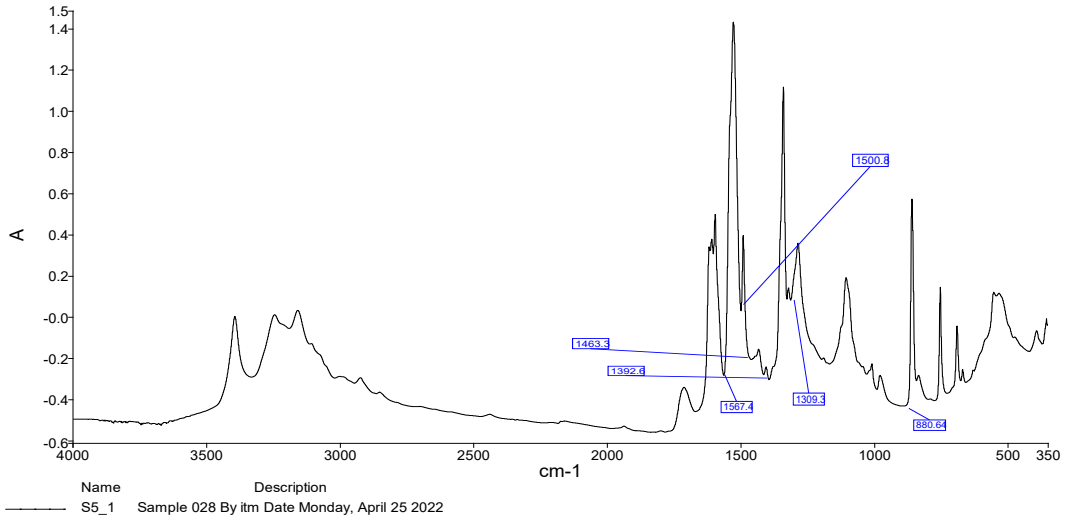

Fig. 5 FT-IR Spectra of Zn S nanoparticles derived from Zn(II) complex.

3.1.3. Magnetic study

A magnetochemical study was carried out in order to determine the presence of interaction between Zn atom in complex. The magnetic moment of Zn complex was measured in order to determine the oxidation state of Zn ions. The Zn (II) complex turned out to be diamagnetic in nature due to the presence of parried electrons in its 3d orbitals.

3.2. Study of Substances in solution

3.2.1. Molar electrical conductivity

Molar conductivity values have been measured for 1mM solution of synthesized Zn (II) complex in DMSO solvent. Molar conductivity value of Zn complex is 55 Ω^{-1} cm^{-1} mol^{-1} which indicates that the Zn(II) complex showed electrolytic behavior[40]. It means that in Zn(II) complex, the corresponding anions (Cl^{-1}) are substituted with solvent molecules during dissolution process. DMSO molecules shifts the equilibrium toward the removal of Cl^{-1} ions from the inner sphere of Zn (II) complex.

3.2.2. UV-visible spectra

UV- Visible spectrum of 0.1mM DMSO solution of ligand contains a maximum peak at 329nm. The corresponding spectrum of Zn (II) complex contains two maximum peaks at 325 and 398 nm. Thus, by comparing the results of the UV –Visible spectra of the Zn complex and the initial thiosemicarbazone ligand in the 0.1 Mm DMSO solution, it can be concluded that thiosemicarbazone moiety remains coordinated to the corresponding zinc metal ions when dissolved in DMSO [41]. In the UV-Vis spectrum, Zn S nanoparticles showed absorption peak at 340 nm. This is a very useful and reliable technique for the primary identification for synthesis of nanomaterials.

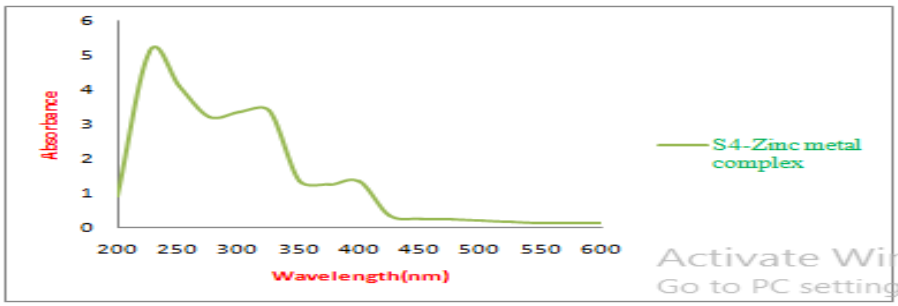

Fig. 6. UV-Visible spectra of Zinc (II) complex.

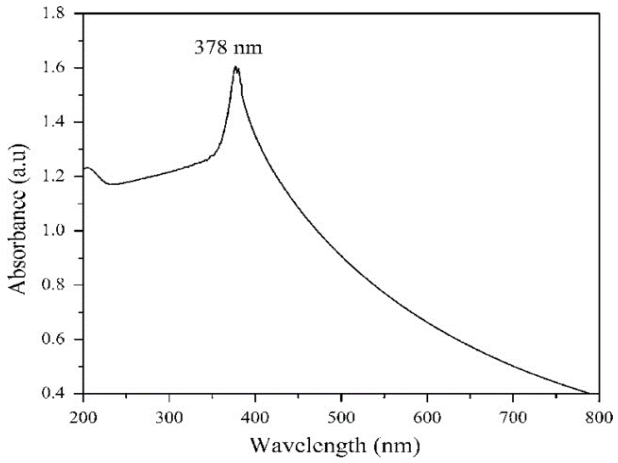

Fig. 7. UV-Visible spectra of biogenic Zn S nanoparticles.

3.2.3. SEM analysis Zn S nanoparticles

The field emission SEM measurement was carried out to get insight into the surface morphology of Zn S nanoparticles. The obtained FESEM micro graph is shown in figure. 9 which demonstrates particles agglomerated in a nano scale while particle was formed in a uniform manner of shape and size i.e. Cubes and spherical shapes and calculated averaged particle sizes of 2.36 nm.

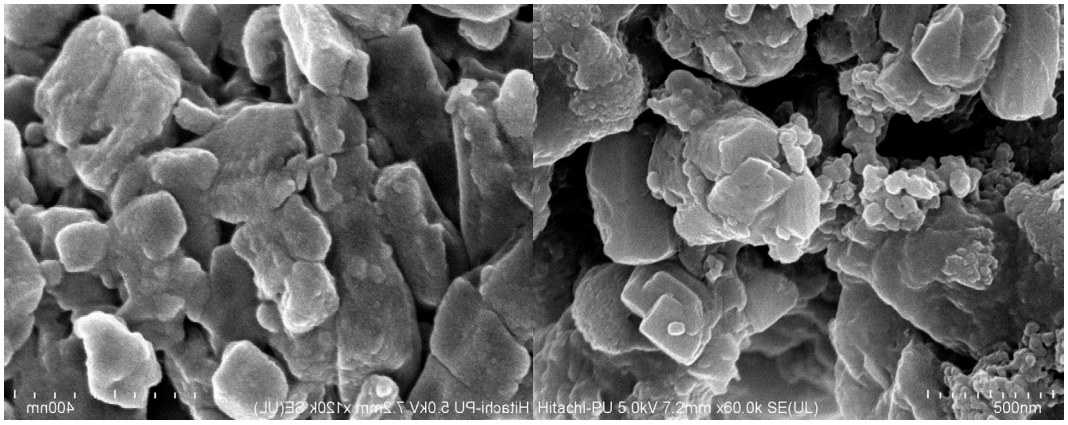

Fig. 8. SEM Images of Zinc Sulfide nanoparticles.

3.2.4. Thermal studies (TGA/DTA) of Zn(II) complex

Thermal decomposition studies of inorganic metal complexes have been received considerable attention now-a-days because it can be used in the structural and kinetic investigation of coordination compounds. The TG-DTA curves of the ligand and its Zn(II) complexes show mainly three stages in the decomposition process (Fig.7). The TGAcurves showed a weight loss initially in the range of 276.93°c with a mass loss of 93.77% indicates the presence of a lattice water molecules. The TG curve of Zn (II) complex exhibited no mass loss between 70°c and 150°c confirms the absence of coordinated water molecules [40]. Weight loss at decomposition temperature in the range of 160.65°c (26.24%) and 259.10°c (84,4%) which corresponds to the loss of amide and chloride ions. The decomposition temperature in the range of 445.46c°c with a mass loss of 49.69% which correspond to the loss of remaining organic moiety of the ligand and finally the copper complex is converted into its oxide [42].

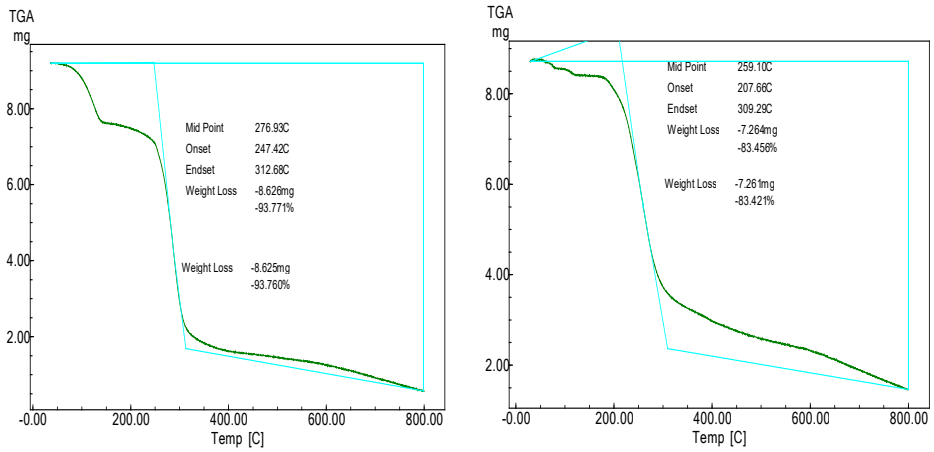

Fig. 9 TGA graphs of a) Schiff base ligand b) Zn(II) complex of Schiff base ligand.

3.3. Biological activity

3.3.1. Antiprolifiraferative activity

The antiprolifirative activity of thiosemicarbazone ligand, its Zinc (II) complex and Zn S nanoparticles have been tested towards human breast cancer cell lines MCF-7. As it can be seen in Table 2. The position of nitrogen atoms in thiosemicarbazone ligand has a tremendous influence on their antiprolifirative activity. The nature of the central atom has a major influence on the antiprolifirative activity of the complex. The activity of Zn NPs towards MCF-7 cells greater than

the activity of the free ligand (L) and its Zn(II) complex due to high surface –volume ration of nanoparticles. In our experiment,normal healthy skin cell lines used as standard for comparison purpose.

Table 2. Antiprolifirative activities of synthesized compounds against human breast cancer cell lines (MCF-7).

S,N.	Test substance	Concentrations ($\mu g/ml$)	Percentage Cytotoxicity after treatment	CTC_{50} ($\mu g/ml$)
1.	Thiosemicarbazone Ligand	1000 500 250 125 62.5 31.25 15.625. 7.8	74.68 ± 2.66 75.22 ± 0.36 76.33 ± 0.89 66.84 ± 5.18 54.48 ± 3.66 39.20 ± 3.24 38.36 ± 2.2 25.60 4.36	75.65
2.	Coordinated Zn (II) Complex	1000 500 250 125 62.5 31.25 15.625. 7.8	75.60 ± 2.60 76.24 ± 0.39 77.90 ± 0.86 69.80 ± 5.16	52.65
3.	Zn SNPs 25.10 4.38	54.42 ± 3.68 40.10 ± 3.26 39.60± 3.24 33.68 3.83	75.68± 2.68 76.22 ± 0.38 77.93 ± 0.89 67.54 ± 5.19 54.41± 3.64 39.10 ± 3.22 38.38 ± 2.2 25.05 ± 4.36	49.375

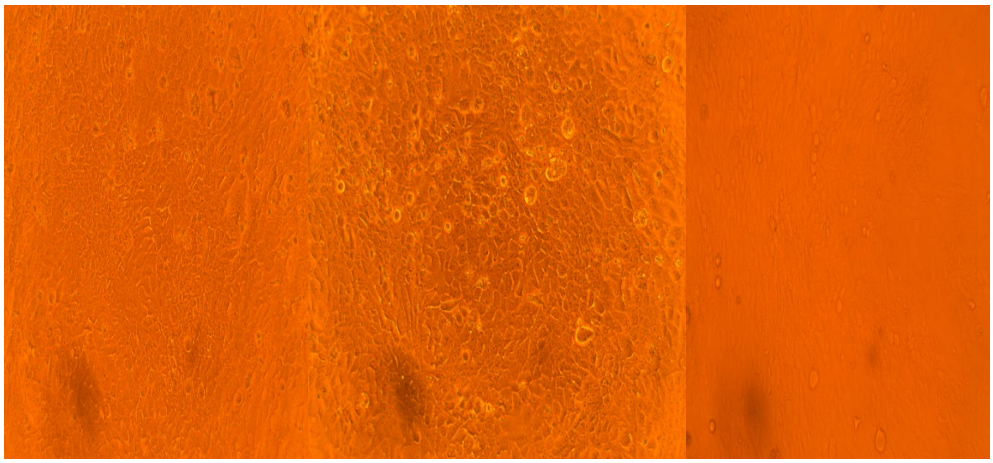

Fig .10 (a) Thiosemicarbazone ligand (b) Zn(II) complex (c) ZnS nanoparticles

3.3.2. Anti- inflammatory activity of compounds

The anti-inflammatory activity of ligand, Zn(II) complex, and ZnS nanoparticle were investigated using the inhibition of albumin denaturation technique, following the method

described by Mizushima et al. with minor modifications. Denaturation of protein is a well-documented cause of inflammation, and the ability of compound to inhibit this process was studies as part of the investigation into the mechanism of anti- inflammatory activity. In this study, Aspiring drug used as standard anti-inflammatory drug at same concentration with maximum inhibition 69.9% in relation to control.

Table 3- Anti- inflammatory activity of compounds

S.N.	Compound	Concentration in µg/ml	Absorption at 210nm	Percentage in inhibition
1.	Control	100	0.733	0%
2.	Thiosemicarbazone ligand(TSC)	100	0.408	55.2%
3.	Zn(II) complex of TSC ligand	100	0.716	65.9%
4.	ZnS nano particles	100	0.746	70.7%
5.	Standard Aspirin drug	100	0.216	69.9%

The inhibitory potential of Zn (II) complex and its ZnS Nano particle showed that the denaturation of protein is a concentration dependent process i.e. as the concentration increases, percentage inhibition also increases. In our study, the ZnS nanoparticles show moderate anti-inflammatory activity as compared to ligand and its Zn(II) complex because zinc is easily oxidized to Zinc ions.. So that Zn S easily diminish free radicals and hydrogen peroxide that produced in inflammation mechanism. [43]. Furthermore, the synthesized Zn S nanoparticles demonstrated a higher anti-inflammatory activity as compared to the standard aspirin drug due to the presence of secondary metabolite like amino acids, phenolic groups in plant extract.

3.3.3. Anti-oxidant activity of compounds

Schiff base ligand, Zn (II) complex and Zn S nanoparticles were screened for antioxidant activity using the DPPH assay. DPPH is a stable free radical compound and has been widely used to test the radical scavenging activity of numerous compounds like herbal and synthetic products. In our study, ZnS nanoparticles showed excellent antioxidant activity than Zn(II) complex & Schiff base ligand. In our experiment ascorbic acid used as a positive control for comparison of antioxidant activities of compounds. The results of antioxidant compounds are in accordance with the theoretical aspects because the anti-oxidant activity was depending upon the number of hydroxyl groups as well as the degree of unsaturation present in compounds. The antioxidant efficiency of compound is directly proportional to the present of total number of –OH groups in benzene ring.

Mechanism of antioxidant activity of Synthesized Compounds:

An unshared electron present on the N atom of DPPH molecule is responsible for the absorbance of light at 517nm and also for formation of visible deep purple colour. When DPPH radical accepts an unpaired electrons donated by an antioxidant compound, the colour of DPPH solution fades, which can be quantitatively measured from the changes in the absorbance of light. The reverse reaction is evaluated by adding DPPH-H at the end of the reaction. If there is an increase in the percentage of remaining DPPH free radical at the plateau, the reaction is reversible, otherwise it is a complete reaction.The DPPH assay evaluates the ability of the compound to donate H to the DPPH radical, resulting in de-colorization of DPPH solution. The greater the de-colorization of solution, the higher the antioxidant activities of compound and this was reflected in a lower IC_{50} value of samples.

Table 4. Troloxa equivalent antioxidant activity of compounds.

S.No.	Compound	DPPH activity IC_{50} $\mu g/ml$
1.	Schiff base ligand [$C_9H_{10}N_4O_2S$]	1.87
2.	$[Zn(C_9H_{10}N_4O_2S)_2]Cl_2$	2.25
3.	Zn S nanoparticles	2.97
4.	Ascorbic Acid (Standard)	3.76

Trolox equivalent antioxidant capacity has been calculated from molar absorptivity by dividing 1.64×10^4.

4. Conclusion

ZnS nanoparticle were successfully prepared from the interaction of synthesized Zn(II0 complex of thiosemicarbazone ligand with aqueous extract of parmotrema perlatum flowers. The Zn(II) complex and its respective adducts contained Zn atom coordinated to the thiosemicarbazone group in N, S, S tridentate fashion. The prepared biogenic ZnS nanoparticles have spherical-shaped morphology with cubic sphalerite phase, which showed size increment with an increase in the bulkiness of the precursor complex. The optical property of the nanoparticles showed a blue shift relative to the band gap energy of bulk ZnS (3.58eV). From various electronic, structural and morphological studies of Zn S, it has been observed that the shape and size of ZnS nanoparticle depends upon the concentration of synthesized Zn(II) complex which was used as a single molecular precursor. The use of fresh aqueous extract of parmotrema perlatum flowers help to decompose Zn(II) complex in a very short time in the spherical shape of ZnS nanoparticle. This is a simple, fast , efficient, ecofriendly and inexpensive method for commercial preparation of ZnS nanoparticles. The use of aqueous extract of flower plays a very important role in reducing reaction time, reducing minimum possibilities of side reactions and prompt conversion of Zn(II) complex into ZnS nanoparticles. This biogenic synthetic method of ZnS nanoparticles has very strong potential to be utilized for large scale industrial production of ZnS nanoparticle. From the resulted of pharmacological activities of compounds, it has been observed that the ZnS nanoparticle can be considered as a good drug candidate for numerous biological applications like anticancer, antioxidant and anti-inflammatory agents in future.

Acknowledgements

The authors would like to extend their gratitude to the Madhya Pradesh Council of Science and Technologies (MPCST) Bhopal, for providing research grant support/ dated 31/03/2023, File No. A/RD/RP-2/347). Authors also acknowledge the Department of Chemistry, School of Sciences, ITM University, Gwalior (M.P.) for providing laboratory facilities.

References

[1] Health MOF, Welfare F. The Ayurvedic Pharmacopoeia of India, Part 1 2001;3:129-30.

[2] Leela K, Anchana Devi C. Isolation, Biosci Biotechnol Res Asia 2017;14:1413-28; https://doi.org/10.13005/bbra/2587

[3] Goyal PK, Verma SK, Sharma AK, Int J Res Ayurveda Pharm 2016;7:102-7; https://doi.org/10.7897/2277-4343.07138

[4] Farooq A, Waheed U. Asian Journal of Biological and Life Sciences. Asian J Biol Life Sci 2012:72-5.

[5] D. D. Perrin, W. L. Armarego, D. R. Perrin, Purification of Laboratory Chemicals, Butterworth-Heinemann, Oxford, UK,2nd edition, 1990.

[6] J. Koaib, N. Bouguila, H. Abassi et al., RSC Advances, vol. 10, no. 16, pp. 9549-9562, 2020; https://doi.org/10.1039/C9RA10284A

[7] U. S. Senapati, R. Athparia, Chalcogenide Letters, vol. 19, pp. 203-216, 2022; https://doi.org/10.15251/CL.2022.193.203

[8] A. Al-Osta, A. Alnehi, A. A. Qaid, H. T. Al-Ahsab, A. Al-Sharabi, Optik, vol. 214, Article ID 164831, 2020; https://doi.org/10.1016/j.ijleo.2020.164831

[9] M. Sathishkumar, M. Saroja, M. Venkatachalam, Optik, vol. 182, pp. 774-785, 2019; https://doi.org/10.1016/j.ijleo.2019.02.014

[10] M. Wu, Z. Wei, W. Zhao, X. Wang, J. Jiang, Journal of Nanomaterials, vol. 2017, Article ID 1603450, 9 pages, 2017; https://doi.org/10.1155/2017/1603450

[11] K. Benyahia, A. Benhaya, M. S. Aida, Journal of Semiconductors, vol. 36, no. 10, Article ID 103001, 2015; https://doi.org/10.1088/1674-4926/36/10/103001

[12] M. Nematollahi, X. Yang, U. J. Gibson, T. W. Reenaas, Thin Solid Films, vol. 590, pp. 28-32, 2015; https://doi.org/10.1016/j.tsf.2015.07.046

[13] A. Mukherjee, P. Mitra, Materials Research, vol. 20, no. 2, pp. 430-435, 2017; https://doi.org/10.1590/1980-5373-mr-2016-0628

[14] P. Kaur, S. Kumar, A. Singh, S. M. Rao, Journal of Materials Science: Materials in Electronics, vol. 26, pp. 9158-9163, 2015; https://doi.org/10.1007/s10854-015-3605-z

[15] N. F. de Andrade Neto, P. M. de Oliveira, M. A. Corrêa, M. R. Bomio Delmonte, F. V. da Motta, International Journal of Applied Ceramic Technology, vol. 18, no. 3, pp. 598-604, 2021; https://doi.org/10.1111/ijac.13718

[16] R. Augustine, A. Hasan, Phytonanotechnology, pp. 195-219, Elsevier, 2020; https://doi.org/10.1016/B978-0-12-822348-2.00011-5

[17] S. H. Ansari, F. Islam, M. Sameem, Journal of Advanced Pharmaceutical Technology & Research, vol. 3, no. 3, pp. 142-146, 2012; https://doi.org/10.4103/2231-4040.101006

[18] M. Alavi, M. R. Hamblin, J. F. Kennedy, Nano Micro Biosystems, vol. 1, no. 1, pp. 15-21, 2022.

[19] M. Alavi, M. Rai, I. R. A. de Menezes, Nano Micro Biosystems, vol. 1, no. 1, pp. 8-14, 2022.

[20] J. M. Baruah, S. Kalita, J. Narayan, International Nano Letters, vol. 9, pp. 149-159, 2019; https://doi.org/10.1007/s40089-019-0270-x

[21] A. Al-Sharabi, A. Alnehia, A. H. Al-Hammadi, K. A. Alhumaidha, A. AL-Osta, Journal of Materials Science: Materials in Electronics, vol. 33, pp. 20812-20822, 2022; https://doi.org/10.1007/s10854-022-08890-7

[22] K. Saravanadevi, M. Kavitha, P. Karpagavinayagam, K. Saminathan, C. Vedhi, Materials Today: Proceedings, vol. 48, Part 2, pp. 352-356, 2022; https://doi.org/10.1016/j.matpr.2020.07.707

[23] M. Alavi, S. Thomas, M. Sreedharan, Micro Nano Bio Aspects, vol. 1, no. 1, pp. 49-58, 2022.

[24]. Khan, M.D.; Malik, M.A.; Akhtar, J.; Mlowe, S.; Revaprasadu, N., Thin Solid Films 2017, 638, 338-344; https://doi.org/10.1016/j.tsf.2017.07.064

[25] Du, X.-S.; Yu, Z.-Z.; Dasari, A.; Ma, J.; Meng, Y.-Z.; Mai, Y.-W., Chem. Mater. 2006, 18, 5156-5158; https://doi.org/10.1021/cm0617135

[26] Lisic, E.C.; Rand, V.G.; Ngo, L.; Kent, P.; Rice, J.; Gerlach, D.; Papish, E.T.; Jiang, X., Open J. Med. Chem. 2018, 8, 30-46; https://doi.org/10.4236/ojmc.2018.82004

[27] Sarker, D.; Hossen, M.F.; Zahan1, M.K.; Haque, M.M.; Zamir, R.; Asraf, M.A.

Synthesis, J. Mater. Sci. Res. Rev. 2020, 5, 15-25; https://doi.org/10.9734/ajacr/2019/v4i430116

[28] Pahontu, E.; Fala, V.; Gulea, A.; Poirier, D.; Tapcov, V.; Rosu, T., Molecules 2013, 18, 8812-8836; https://doi.org/10.3390/molecules18088812

[29] Jing, M.; Li, F.; Chen, M.; Zhang, J.; Long, F.; Jing, L.; Lv, X.; Ji, X.; Wu, T. J. Alloys Compd. 2018, 762, 473-479; https://doi.org/10.1016/j.jallcom.2018.05.224

[30] Mbewana-Ntshanka, N.G.; Moloto, M.J.; Mubiayi, P.K., J. Nanotechnol. 2021, 2021, 6675145. Catalysts 2022, 12, 61 20 of 20; https://doi.org/10.1155/2021/6675145

[31] Onwudiwe, D.C.; Hrubaru, M.; Ebenso, E.E., J. Nanomater. 2015, 9, 143632; https://doi.org/10.1155/2015/143632

[32] Akhtar, M.; Alghamdi, Y.; Akhtar, J.; Aslam, Z.; Revaprasadu, N.; Malik, M.A., Mater. Chem. Phys. 2016, 180, 404-412; https://doi.org/10.1016/j.matchemphys.2016.06.024

[33] Ajibade, P.A.; Sikakane, B.M.; Botha, N.L.; Oluwalana, A.E.; Omondi, B. J. Mol. Struct. 2020, 1221, 128791; https://doi.org/10.1016/j.molstruc.2020.128791

[34] Pal, M.; Mathews, N.R.; Sanchez-Mora, E.; Pal, U.; Paraguay-Delgado, F.; Mathew, X., J. Nanoparticle Res. 2015, 17, 301; https://doi.org/10.1007/s11051-015-3103-5

[35] Yepseu, A.P.; Isac, L.; Nyamen, L.D.; Cleymand, F.; Duta, A.; Ndifon, P.T., J. Nanomater 2021, 2021, 9975600; https://doi.org/10.1155/2021/9975600

[36] Pawar, A.S.; Masikane, S.C.; Mlowe, S.; Garje, S.S.; Akerman, M.P.; Revaprasadu, N., Inorg. Chim. Acta 2017, 463, 7-13; https://doi.org/10.1016/j.ica.2017.04.009

[37] Abdelhady, A.L.; Ramasamy, K.; Malik, M.A.; O'Brien, P.; Haighb, S.J.; Raftery, J., J. Mater. Chem. 2011, 21, 17888-17895; https://doi.org/10.1039/c1jm13277f

[38] Krishna, P.M.; Reddy, N.B.G.; Kottam, N.; Yallur, B.C.; Katreddi, H.R., Sci. World J. 2013, 2013, 828313; https://doi.org/10.1155/2013/828313

[39] Jain, M.; Babar, D.G.; Garje, S.S., Appl. Nanosci. 2019, 9, 353-367; https://doi.org/10.1007/s13204-018-0915-5

[40] Gaber, A.; Refat, M.S.; Belal, A.A.M.; El-Deen, I.M.; Hassa, N.; Zakaria, R.; Alhomrani, M.; Alamri, A.S.; Alsanie, W.F.; Saied, E.M., Molecules 2021, 26, 2288; https://doi.org/10.3390/molecules26082288

[41] Wilson, J.T.; Jiang, X.; McGill, B.C.; Lisic, E.C.; Deweese, J.E., Chem. Res. Toxicol. 2016, 29, 649-658; https://doi.org/10.1021/acs.chemrestox.5b00471

[42] Conner, D.; Medawala, W.; Stephens, M.T.; Morris, W.H.; Deweese, J.E.; Kent, P.L.; Rice, J.J.; Jiang, X.; Lisic, E.C., Open J. Inorg. Chem. 2016, 6, 146; https://doi.org/10.4236/ojic.2016.62010

[43] Sarker, D.; Hossen, M.F.; Zahan1, M.K.; Haque, M.M.; Zamir, R.; Asraf, M.A., J. Mater. Sci. Res. Rev. 2020, 5, 15-25; https://doi.org/10.9734/ajacr/2019/v4i430116